Simulations of magnetic fields generated by the Antarctic Circumpolar Current at satellite altitude: Can geomagnetic measurements be used to monitor the flow?

Frédéric Vivier

Laboratoire d'Océanographie Dynamique et de Climatologie, CNRS UMR 7617 Université Pierre et Marie Curie, Paris, France

Ernst Maier-Reimer

Max Planck Institute for Meteorology, Hamburg, Germany

Robert H. Tyler

Applied Physics Laboratory, University of Washington, Seattle, Washington, USA

Received 24 February 2004; revised 29 April 2004; accepted 3 May 2004; published 27 May 2004.

[1] With a volume transport of $\sim 134 \times 10^6$ m^3/s at the Drake Passage, the Antarctic Circumpolar Current (ACC) is the strongest ocean current. In the interest of estimating the secondary magnetic fields generated by the magnetohydrodynamic interaction of this flow with Earth's main field, we compare numerical results for the magnetic fields obtained using flow from three different ocean general circulation models. These simulations all expect detectable ocean signals in the magnetic records at ground and satellite altitude (400 km). The variability of this contribution is highly correlated with the ACC transport, a very important variable for climate studies. Observed magnetic fields could then be used, in principle, to derive an index of variability of the ACC. However given its small amplitude compared with other magnetic contributions, extracting the ocean's signal from observations remains a challenge at this time. *INDEX TERMS:* 4512 Oceanography: Physical: Currents; 3005 Marine Geology and Geophysics: Geomagnetism (1550); 4294 Oceanography: General: Instruments and techniques; 1635 Global Change: Oceans (4203); 1555 Geomagnetism and Paleomagnetism: Time variations—diurnal to secular. **Citation:** Vivier, F., E. Maier-Reimer, and R. H. Tyler (2004), Simulations of magnetic fields generated by the Antarctic Circumpolar Current at satellite altitude: Can geomagnetic measurements be used to monitor the flow?, *Geophys. Res. Lett.*, *31*, L10306, doi:10.1029/2004GL019804.

1. Introduction

[2] With a typical conductivity σ of $3-4$ S m^{-1}, seawater is a fairly good electrical conductor. As the ocean fluid flows through the earth's main magnetic field $\boldsymbol{F}$, electric currents and associated magnetic fields $\boldsymbol{b}$ ($\|\boldsymbol{b}\| \ll \|\boldsymbol{F}\|$) are generated through a magnetohydrodynamic process often called "motional induction". Substantial effort for the oceanic application began in the mid-1900s with a focus on inferring ocean flow from in situ electric field observations [e.g., *Sanford*, 1971]. Optimism toward the potential for inferring flow from remote magnetic observations is much more recent [e.g., *Tyler et al.*, 1997, 1999]. While it has now been shown that ocean generated magnetic signals (so far due to tides) can be detected in land [e.g., *McKnight*, 1995] and, recently, satellite magnetometer records [*Tyler et al.*, 2003], the oceanic signals are small in comparison to other contributions (mainly from the core but also due to sources in the ionosphere, magnetosphere, and lithosphere) which are only recently becoming mapped with sufficient accuracy [e.g., *Sabaka et al.*, 2002] to attempt resolving the smaller oceanic contributions.

[3] The Antarctic Circumpolar Current (ACC) is the strongest ocean current of the World Ocean: it transports ~ 130 Sv (Sv = 10^6m^{3}s^{-1}) of water around Antarctica, which makes it the most significant exchanger of heat, salt, and momentum between the Atlantic, Indian and Pacific oceans. The ACC is an essential link of the global meridional overturning circulation, which has critical implication for the Earth's climate. Its strength may influence the magnitude of the thermohaline circulation and hence impact global climate [e.g., *Mikolajewicz et al.*, 1993; *Toggweiler and Samuels*, 1995]. The ACC transport is therefore a key climatic index, and its monitoring is a high priority for the climate community.

[4] In this contribution our motivation is twofold: Our primary interest is to examine the capacity of geomagnetic observations both at the sea level and at satellite altitude to provide an index of variability for the ACC. Our second motivation is to contribute to the geophysical community engaged in mapping the various components of the earth's magnetic field by providing estimates of the small oceanic contribution. It is now regarded that resolution of the oceanic magnetic contribution will help improve mapping of both oceanic and even the larger non-oceanic contributions. This letter provides estimates of magnetic signals due to low-frequency (<0.2 cycles per day (cpd)) ocean variability.

[5] Here, we numerically calculate and examine the magnetic signature of ocean flows prescribed from three different ocean general circulation models (OGCM). This "ensemble" view identifies the robust features vs. model dependent ones. Although magnetic fields are estimated for the World Ocean, we will focus on the Southern Hemi-

0094-8276/04/2004GL019804$05.00

sphere, where the magnitude of the fields is largest, and on the relationship between the ACC transport and the magnetic field variability. Section 2 presents the formulation for calculating the magnetic field. In section 3, we present the results of the three numerical experiments forced with different simulated ocean flows, while we discuss these results in section 4.

2. A 2-D Induction Equation

[6] The formulation used is the same as that by *Tyler et al.* [1997] [see also *Price*, 1949]. It is based on a "thin-shell" approximation for the flow as well as for any electric currents. This leads to the neglect of vertical (i.e., radial) velocities compared with horizontal velocities $\boldsymbol{u}_H$ (subscript H denotes the horizontal component hereafter). For the electric currents, this approximation requires a more weakly justifiable assumption that regions above and below the shell are electrical insulators. The lower atmosphere ($\sigma \sim 10^{-14}$ S m^{-1}) can clearly be treated as an insulator. We allow the thin conductive shell to include both the ocean as well as a conductive layer of sediments. (The global distribution of sediment conductance is derived using the method of *Everett et al.* [1999] based on sediment thicknesses of *Laske and Masters* [1997].) The upper region of the earth's mantle is typically two to three orders of magnitude less conductive than seawater or sediments [*Parkinson and Hutton*, 1989] and hence treating it as an insulator would seem reasonable. There are, however, potential pitfalls in this assumption, that cannot be accurately addressed because of limited knowledge of the conductivity structure of the solid earth. Indeed, inductive coupling between electric currents in the thin shell and highly conductive regions in the lower mantle are potentially important for the most rapid of the low-frequency ocean flow but are here ignored while assuming in our formulation that the electric currents remain in nearly static balance with their sources.

[7] Ampere's Law and Ohm's Law can be combined and integrated over the thin shell h as

$$-\int_h \partial_z \boldsymbol{b}_H \times \hat{\boldsymbol{z}} dz = \mu_0 \int_h \boldsymbol{J}_H dz = \mu_0 \int_h (\sigma \boldsymbol{E}_H + \sigma \boldsymbol{u}_H \times F_z \hat{\boldsymbol{z}}) dz, \tag{1}$$

where $\hat{\boldsymbol{z}}$ is the unit vertical vector, and $\boldsymbol{E}_H$ is the horizontal electric field, $\boldsymbol{J}_H$ is the horizontal electric current density, and the forcing term on the right involves the depth integrated conductivity transport (taken from one of three different OGCMs) and the main field F_z (taken from the CO2 model [*Holme et al.*, 2003]). With the steady-state assumption, we then replace the first term in the first integral on the far right with $-\Sigma \nabla_H \phi$ where ϕ is the electric potential (averaged over the depth h) and the conductance Σ is the integral of conductivity over h which embraces the oceans and sediments. We then divide (1) by Σ before taking the curl to remove the $\nabla\phi$ term. Because charge is conserved, the middle equality in equation (1) is non-divergent and can be written as a stream function ψ_e for the depth integrated electric currents (i.e., $\int_h \boldsymbol{J}_H dz = \nabla\psi_e \times \hat{z}$) which allows us to write the following scalar governing equation for ψ_e:

$$\nabla \cdot \left(\Sigma^{-1} \nabla \psi_e\right) = \nabla \cdot \left(\Sigma^{-1} F_z \int_h \sigma \boldsymbol{u}_H dz\right). \tag{2}$$

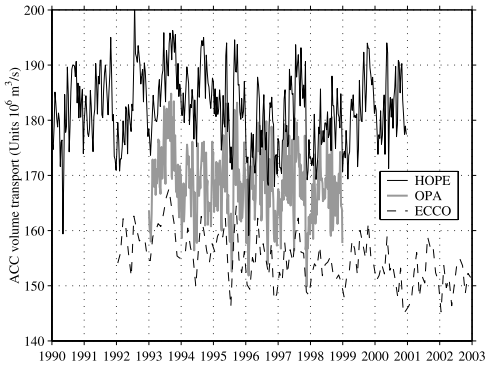

Figure 1. ACC volume transport in Drake Passage, between Chile and Antarctica, from the three ocean models. See color version of this figure in the HTML.

[8] Once (2) has been solved over the whole sphere to obtain ψ_e, we calculate the magnetic field associated with these electric currents. In the insulating regions, the magnetic field is irrotational and can be written as $\boldsymbol{b} = -\nabla M$. Because it is also non-divergent, $\nabla^2 M = 0$. This equation for M can be solved in the region above the ocean under the condition that $M \rightarrow 0$ for large distance above the ocean. The lower boundary condition for M at the sea surface is obtained from the solution ψ_e noting that by symmetry $\boldsymbol{b}_H(z = -h) = -\boldsymbol{b}_H(z = 0)$ in which case we can set $M = \frac{\mu_0}{2}\psi_e$. (This relationship can be obtained from the first equation in equation (1) and the requirement that $M(z = 0)$ remain continuous.) The symmetry relationship invoked above is strictly valid for planar geometry, but is expected to be a reasonable assumption for this study involving electric current loops of smaller scale than a great circle.

3. Simulated Magnetic Fields

[9] We compare simulations from three experiments forced with the flows from three OGCMs: OPA, HOPE, and ECCO. All three are primitive equation models that produce the 3D velocity field as well as thermohaline variables. They differ by many aspects including their forcing, resolution, and turbulent closure schemes for mixing. OPA 8.1 is developed at LODYC [*Madec et al.*, 1998]. We used products from a 2° -resolution, 31 vertical levels, global run, forced with National Center for Environmental Predictions (NCEP) surface fluxes, and satellite winds. In the configuration used here, HOPE (Hamburg Ocean Primitive Equation) [e.g., *Marsland et al.*, 2003] has 13 vertical levels, a horizontal resolution of 2° and is forced with NCEP. ECCO is based on the Massachussetts Institute of Technology OGCM and assimilates TOPEX/Poseidon altimeter data. The ECCO-1 data used corresponds to a 1° -horizontal resolution and 46 vertical levels setting.

[10] The volume transport of the ACC in Drake Passage is a useful index to compare the performances of the

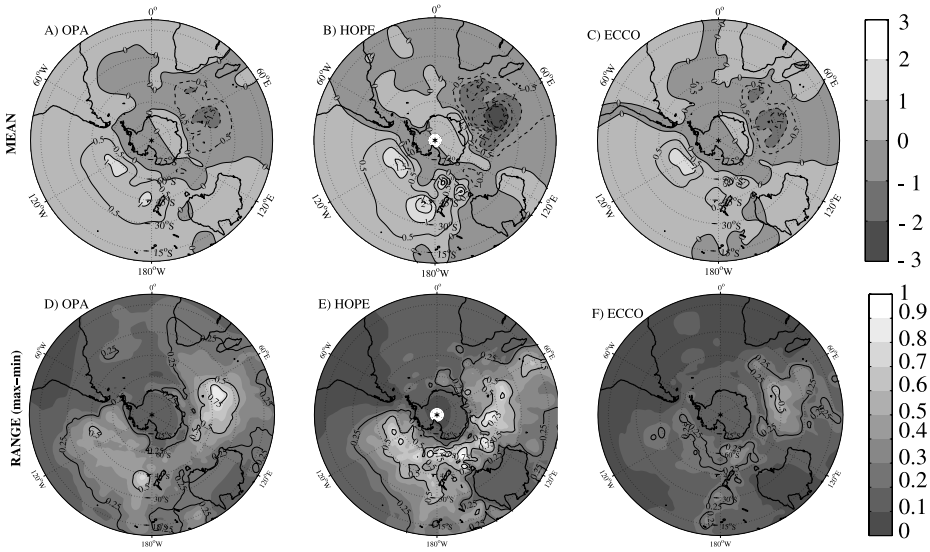

Figure 2. Scalar anomaly b_F of the magnetic field generated by ocean flows at CHAMP satellite altitude (400 km). The first row of panels is the mean field from different forcing flows: (a) OPA, (b) HOPE, and (c) ECCO. The second row of panels is the range of variability (peak to peak amplitude). Units are nT. See color version of this figure in the HTML.

different models (Figure 1). OPA, HOPE, and ECCO have a mean transport of 168, 182 and 155 Sv, respectively with a standard deviation of 6.4, 6.6 and 4.6 Sv, respectively. The mean ACC transport was measured at 134 Sv with a standard deviation of 10.3 Sv [*Whitworth and Peterson*, 1985]. Hence all models tend to overestimate the mean flow while underestimating the variability of the ACC. The transport was found to be steady over the past 25 years [*Cunningham et al.*, 2003]: the trend given by ECCO is probably an artifact.

[11] In the following, we discuss the component of $\boldsymbol{b}$ in the direction of the main field $\boldsymbol{F}$, denoted b_F. This scalar anomaly is in practice what is measured by scalar magnetic instruments [*Olsen et al.*, 2000]. The means and the standard deviations of b_F, at satellite altitude, are shown in Figure 2, while the other components of the fields have similar order of magnitude (not shown). The mean $\langle b_F \rangle$ is on the order of 1 to 2 nT (Figures 2a–2c) and is largest for the HOPE model, which has the largest ACC transport. Figure 2c is consistent with an estimate obtained by the *Swarm Team* [2004]. Maps of $\langle b_F \rangle$ are dominated by two cells, one positive in the Pacific ocean, one negative in the Indian ocean, located east and west of the south magnetic pole. These regions of large forcing are regions where the ACC is orthogonal to isocontours of F_z. This can be understood because a systematic contribution to the forcing term (on the right of (2)) over large scales is primarily just the advection of F_z. Indeed, large-scale low-frequency ocean flows are predominantly nondivergent, and the conductivity transport (integral in (2)) is also approximately nondivergent. Flow across Σ contours is important locally but does not contribute systematically over large scales.

[12] At the earth's surface, not surprisingly, $\langle b_F \rangle$ is larger, ranging from -4 to 4 nT for OPA (not shown) and has shorter spatial scales, unaltered by geometrical attenuation.

[13] The variability of simulated b_F is $\lesssim$0.2 nT rms at satellite altitude but the range of variation is $\lesssim$1 nT (Figures 2d–2f). Although these numbers probably underestimate the actual variability of b_F, it is worth mentioning that the mean b_F is large enough to be detectable from satellite-borne magnetometers such as those aboard Oersted [*Neubert et al.*, 2001] and CHAMP [*Reigber et al.*, 2002]. The weaker variability could eventually be detected (the resolution of the scalar instrument is 0.1 nT), but this would likely require more advanced magnetic missions such as Swarm [*Swarm Team*, 2004], one of the many goals precisely is to try and recover the magnetic signature of the oceans.

[14] In order to examine to what extent the variability of b_F can be related to the variability of the ACC, we

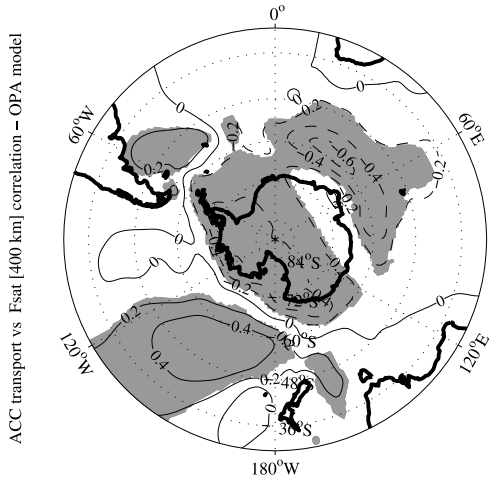

Figure 3. Correlation coefficient (significant at 95% in shaded areas) between b_F, the scalar anomaly of the magnetic field, at 400 km and the ACC volume transport in Drake passage. See color version of this figure in the HTML.

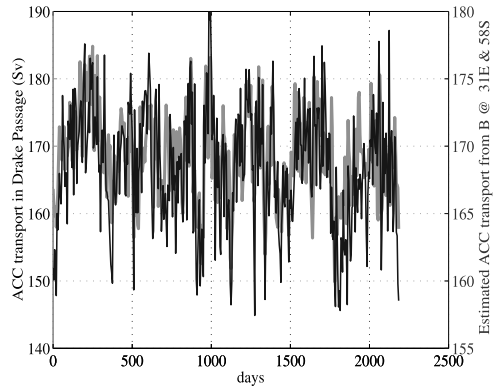

Figure 4. ACC volume transport from OPA model in Drake Passage (gray line) and estimated transport obtained by linear regression of the simulated magnetic field b_F at 31°E and 58°S, at satellite altitude (black line). See color version of this figure in the HTML.

systematically examine the correlation coefficient between the volume transport in Drake Passage and b_F at every location (Figure 3). This figures exhibits regions of high correlations in the South Pacific and in the Argentine basin, and regions highly anticorrelated (up to -0.7) in the Indian Ocean and along Antarctica. Finding significant correlations at regions remote from Drake Passage can be explained by the fact that the leading mode of seasonal variability of the ACC is circumpolarly uniform [e.g., *Hughes et al.*, 1999].

4. Summary and Conclusion

[15] Based on 3 state-of-the-art ocean models, we have estimated the magnetic field generated by the ocean both at the earth's surface, and at the altitude of the CHAMP satellite (400 km). The mean magnetic field is largest in the Southern Hemisphere and is mainly due to the eastward flowing ACC: it reaches up to $\sim$5 nT in some locations of the earth's surface with a variability of up to 2 nT rms. At an altitude of 400 km, the mean magnetic field reaches 1–2 nT, while the simulated variability reaches $\sim$0.2 nT rms with a range of $\lesssim$1 nT. However, this value is likely to be an underestimate as the ACC transport variability simulated by the 3 OGCMs is 40 to 50% smaller than what was observed. A first conclusion of this study is that the magnetic signal generated by low-frequency (<0.2 cpd) ocean flows is within the range of capabilities of satellite-borne sensors, and is hence in theory detectable.

[16] In addition, we find that such magnetic field is, in some regions, highly correlated with the ACC transport. Consequently one could use the former, be it measured from satellites or from observatories at the ground (where stronger signals are expected), as an index of variability of the latter. This would be an invaluable application given the difficulty to obtain integral measurements of the flow in general, and at these remote latitudes in particular. An estimate of the ACC transport obtained by linear regression of b_F is shown in Figure 4.

[17] In summary, any attempt to extract an index of ACC variability from magnetic data remains highly motivated. The difficulty in separating the ocean signals from other contributions to the geomagnetic fields is however real: not only is the signal-to-noise ratio (SNR) small but there is, unlike for the case of the tides [*Tyler et al.*, 2003], no phase-locked frequency of variation. The ACC varies on a wide range of frequencies from days to decades and so do most contributions to the external field, although specific spatial characteristics of the ocean signal may help in separating this contribution. There are however reasons to remain optimistic: modeling of the various contributions to the geomagnetic field are becoming increasingly accurate [*Sabaka et al.*, 2002], and decisive progress can be expected from future magnetic missions such as Swarm [*Swarm team*, 2004]. The small SNR is not necessarily damning per se: satellite altimetry, with typical SNR of 10^{-4}, is nonetheless routinely and successfully used in oceanography.

[18] **Acknowledgments.** RT gratefully acknowledges support for this study from the NASA and the ONR. FV thanks J. Sirven (LODYC) for his help in formulating the 2D iterative spherical harmonics model for ψ_e, G. Madec, A. Bozec and R. Hordoir for making OPA products available. We are grateful to the ECCO Consortium (http://www.ecco-group.org/), for making their products available. We sincerely thank R. Holme and G. Hulot, who reviewed this manuscript, for their valuable comments.

References

Cunningham, S. A., S. G. Alderson, B. A. King, and M. A. Brandon (2003), Transport and variability of the Antarctic Circumpolar Current in Drake Passage, *J. Geophys. Res.*, *108*(C5), 8084, doi:10.1029/2001JC001147.

Everett, M. E., S. Constable, and C. Constable (1999), Modelling three-dimensional induction effects in satellite data, paper presented at the 2nd International Symposium on Three-Dimensional Electromagnetics, Univ. of Utah, Salt Lake City, 16–20 Oct.

Holme, R., N. Olsen, M. Rother, and H. Lühr (2003), CO_2—A CHAMP magnetic field model, in *Proceedings of the First CHAMP Science Meeting*, edited by C. Reigber, H. Lühr, and P. Schwintzer, Springer-Verlag, New York.

Hughes, C. W., M. P. Meredith, and K. J. Heywood (1999), Wind driven transport fluctuations through Drake Passage: A southern mode, *J. Phys. Oceanogr.*, *29*, 1971–1992.

Laske, G., and G. Masters (1997), A global digital map of sediment thickness (abstract), *Eos Trans. AGU*, *78*(46), Fall Meet. Suppl., F483.

Madec, G., P. Delecluse, M. Imbard, and C. Lévy (1998), OPA 8.1 ocean general circulation model reference manual, in *Note du Pôle de Modélisation*, p. 91, Inst. Pierre-Simon Laplace, Paris.

Marsland, S., H. Haak, J. H. Jungclaus et al. (2003), The Max-Planck-Insitute global ocean sea/ice model with orthogonal curvilinear coordinates, *Ocean Dyn.*, *5*, 91–127.

McKnight, J. D. (1995), Lunar daily geomagnetic variations in New Zealand, *Geophys. J. Int.*, *122*, 889–898.

Mikolajewicz, U., E. Maier-Reimer, T. J. Crowley, and K.-Y. Kim (1993), Effect of Drake and Panamanian gateways on the circulation of an ocean model, *Paleoceanography*, *8*, 409–426.

Neubert, T., M. Mandea, G. Hulot et al. (2001), Ørsted satellite captures high-precision geomagnetic field data, *Eos Trans. AGU*, *82*(8), 81, 87–88.

Olsen, N., et al. (2000), Ørsted Initial Field Model, *Geophys. Res. Lett.*, *27*, 3607–3610.

Parkinson, W. D., and V. R. S. Hutton (1989), The electrical conductivity of the Earth, in *Geomagnetism*, vol. 3, edited by J. A. Jacobs, pp. 261–232, Academic, San Diego, Calif.

Price, A. T. (1949), The induction of electrical currents in non-uniform thin sheets and shells, *Q. J. Mech. Appl. Math.*, *2*, 283–310.

Reigber, C., H. Luhr, and P. Schwintzer (2002), Champ mission status, *Adv. Space Res.*, *30*, 129–134.

Sabaka, T. J., N. Olsen, and R. A. Langel (2002), A comprehensive model of the quiet-time, near-Earth magnetic field: Phase 3, *Geophys. J. Int.*, *151*, 32–68.

Sanford, T. B. (1971), Motionally induced electric fields in the sea, *J. Geophys. Res.*, *76*, 3476–3493.

Swarm Team (2004), Swarm, the Earth's magnetic field and environment explorers, in *Report for Mission Selection*, *Rep. SP-1279(6)*, ESA Publ., Noordwijk, Netherlands.

Toggweiler, J. R., and B. Samuels (1995), Effect of Drake Passage on the global thermohaline circulation, *Deep Sea Res., Part I*, *42*, 477–500.

Tyler, R. H., L. A. Mysak, and J. M. Oberhuber (1997), Electromagnetic fields generated by a three dimensional global ocean circulation, *J. Geophys. Res.*, *102*, 5531–5552.

Tyler, R. H., J. M. Oberhuber, and T. B. Sanford (1999), The potential for using ocean generated electromagnetic fields to remotely sense ocean variability, *Phys. Chem. Earth, Part A*, *24*, 429–432.

Tyler, R. H., S. Maus, and H. Lühr (2003), Satellite observations of magnetic fields due to ocean tidal flow, *Science*, *299*, 239–241.

Whitworth, T., and R. G. Peterson (1985), Volume transport of the Antarctic Circumpolar Current from bottom pressure measurements, *J. Phys. Oceanogr.*, *15*, 810–816.

E. Maier-Reimer, Max Planck Institute for Meteorology, Bundesstrasse 55, D-20146 Hamburg, Germany.

F. Vivier, LODYC, Tour 45-55 4E, 4 place Jussieu, F-75005 Paris, France. (fvi@lodyc.jussieu.fr)

R. H. Tyler, Applied Physics Laboratory, University of Washington, 1013 NE 40th Street, Seattle, WA 98105-6698, USA.